

A zero-field electron spin resonance spectrometer for the study of transient radical ion pairs

C R Timmel¹, J R Woodward¹, P J Hore¹, K A McLauchlan^{1,3}
and D V Stass²

¹ Physical and Theoretical Chemistry Laboratory, Oxford University, South Parks Road, Oxford OX1 3QZ, UK

² Institute of Chemical Kinetics and Combustion, Novosibirsk 630090, Russia

E-mail: kamcl@physchem.ox.ac.uk

Received 11 January 2001, accepted for publication 1 March 2001

Abstract

A zero-field electron spin resonance spectrometer is described for measuring the spectra of spin-correlated radical ion pairs in solution in the frequency range 1–80 MHz. The radical ions are created by continuous optical irradiation and rapidly recombine to form an exciplex whose fluorescence is monitored as the radiofrequency is swept, also continuously. The probability of recombination depends upon the singlet character of the radical pair at the time that the radicals re-encounter after an initial separation in the formation step. This is affected directly by resonant state mixing induced within the radical pair energy manifold by the applied radiofrequency field. The method yields the spectrum of the radical pair and also allows direct observation of the effects of radiofrequency radiation on the yields of products formed from radical combination reactions.

Keywords: electron spin resonance, zero-field, radical ion pairs, radiofrequency spectrometer, oscillating magnetic field effects

1. Introduction

It is well known that the yields of radical combination reactions in solution may be affected by static magnetic fields as a result of radicals being produced in pairs [1]. Since reaction occurs with conservation of spin multiplicity a 'spin-correlated radical pair' (SCRIP) is formed in a quantum state that is not usually a stationary state of the system. Reaction of a molecule in a singlet state, for example, yields a singlet-correlated pair that subsequently acquires triplet character through state mixing, normally under the hyperfine interactions. This influences the subsequent reactivity since bond formation to yield products depends upon the singlet character of the pair. Application of an external static magnetic field influences the energy levels of the SCRIP and affects the efficiency of the mixing process. At very low field strengths the mixing times are long compared with the lifetime of the radical pair in normal liquids and field effects are seen only if the pair is constrained to stay together, for example by Coulombic

interactions between radical ions [2–4]. It has recently been demonstrated, experimentally [5, 6] and theoretically [7, 8], that the yields can also be affected by irradiation with external radiofrequency fields resonant at the hyperfine frequencies, which lie in the range 0–100 MHz for proton couplings in organic radicals. This allows measurement of the mixing frequencies, identification of the radicals forming the pair, and interpretation to yield the dynamics of the system. The experiment also provides the first direct evidence that chemical reaction yields can be affected by radiofrequency radiation, and may be relevant to the (unconfirmed) reports of the effects of such radiation in biology, including humans, where radical reactions are common.

Theory suggests that the effect is largely independent of the precise chemical nature of the radicals and a convenient system can be chosen for investigation, knowing that it has general significance [7]. In common with several previous radical pair studies we use a reaction between the singlet excited state of an aromatic hydrocarbon (for instance pyrene, Py), produced by light absorption, and an electron acceptor (for instance dicyanobenzene, DCB) to yield a pair of radical

³ To whom correspondence should be addressed at the above address.

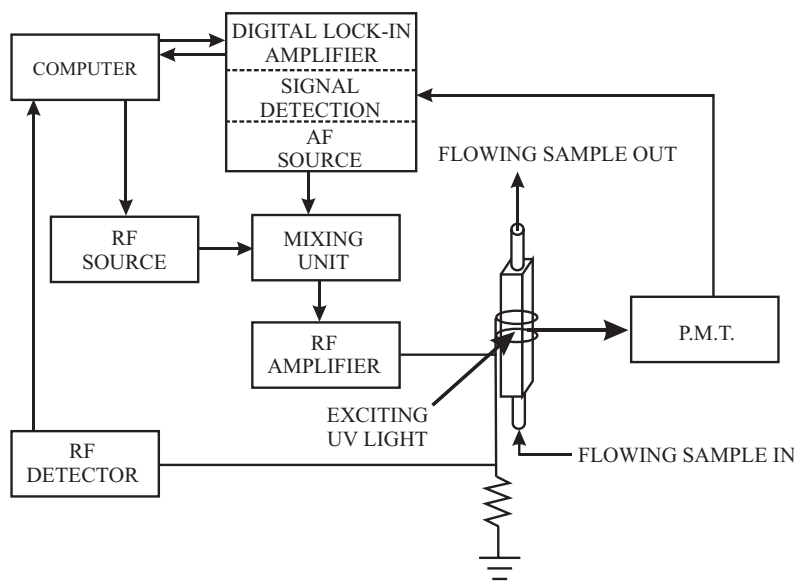
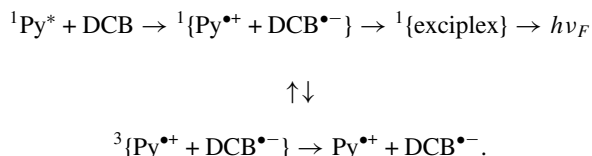


Figure 1. A basic block diagram of the spectrometer. Light from a xenon lamp (not shown) creates radicals inside a coil to which RF radiation is applied in the frequency range 1–80 MHz. The RF is 100% amplitude modulated at an audiofrequency (AF) in a mixer so that a proportion of the fluorescent light that results from an exciplex formed on radical recombination is itself modulated. It is detected by a photomultiplier tube (PMT) whose output varies at the modulation frequency and is applied to a phase sensitive ('lock-in') detector whose dc output constitutes the observed signal. The modulated RF is fed to the coil and then to a dummy load for impedance matching. The RF level is detected across the load and the resulting dc signal is fed back to the computer as a part of a loop which ensures that the RF power level applied to the sample is independent of the frequency, and that the circuitry has a flat frequency response. The details are shown in figures 2 and 4. The sample is pumped continuously through the irradiation region.

ions [1, 9]. For our purposes the complex reaction scheme can be simplified to



It is only the singlet \leftrightarrow triplet inter-conversion that is affected by the field. The main product of the radical re-combination, which occurs mostly through the singlet state of the SCRPs, is a singlet exciplex that fluoresces and returns the molecules to their ground states. Competing processes, which cause not all the triplet SCRPs to revert to the singlet state and are crucial to observe a field effect, are diffusion of radical ions from it (as shown) and recombination through the triplet state.

In the experiment described below the sample is subject to an oscillating radiofrequency (RF) magnetic field whilst under continuous irradiation from a xenon lamp to produce the radicals. The effect of the RF field on the product yield is monitored by observing the fluorescence intensity as the frequency of the RF radiation is changed. The fluorescence is detected in an orthogonal direction to the exciting light to make this a sensitive zero-background measurement. The experiment is performed without a static magnetic field applied and yields the zero-field electron spin resonance (ESR) spectrum of the radical pair. The more recent previous zero field ESR studies have involved observations of transition metal ions [10–12] and of electron spin echo modulation in low temperature solids [13], whilst zero-field NMR appears to have been last reviewed in 1987 [14].

2. The apparatus

2.1. An overview

The creation of free radicals by optical irradiation and the observation of fluorescence from a reaction are well established and pose few problems in instrument design in the apparatus described below. But the requirement to subject the sample simultaneously to RF radiation of sufficient intensity to produce the effects sought whilst sweeping it from 1–80 MHz (see below) at constant field strength is not straightforward, and it is this that requires most attention. It has proved possible using a feed-back loop that is described below. The magnitude of the field effect is expected to be low, possibly leading to a few per cent variation of total fluorescence intensity at resonance, and to improve the signal-to-noise ratio the RF is 100% amplitude modulated at a low audiofrequency (AF). This causes that part of the fluorescence that is affected itself to be modulated, and enables narrow-band phase-sensitive detection. This method, used in a previous experiment in which the frequency was not swept continuously [5], implies that a signal is observed only if the RF influences the reaction, an important direct indication that it does so. A consequent requirement of the experiment is that the modulation depth should not vary as the RF frequency is swept.

A simple block diagram of the equipment is given in figure 1 and its component parts are described below. An inter-connection diagram between the various units is provided in figure 2 whilst the details of the spectrometer block and a photograph of its lid showing the construction of the RF coil are shown in figure 3.

The Stanford Instruments SR830 digital phase-sensitive detector employed conveniently includes a sine-wave

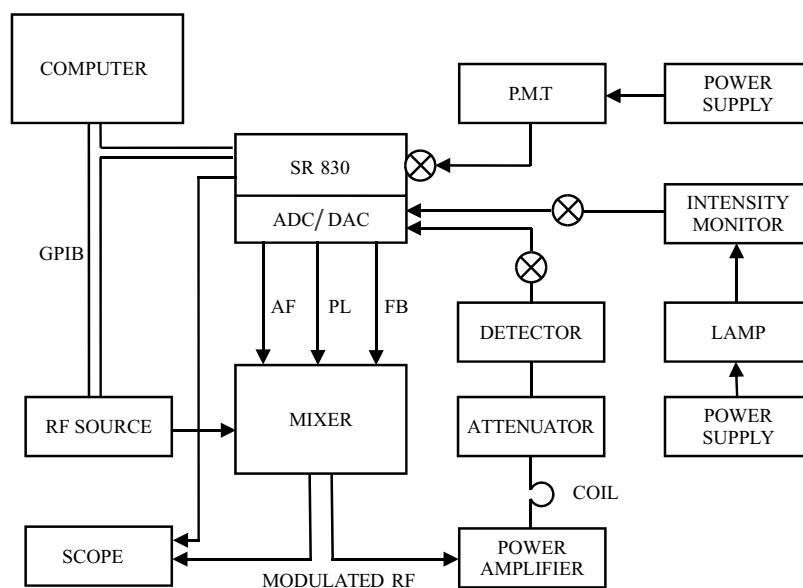


Figure 2. A simplified inter-connection diagram. As described in the text, advantage is taken of the existence of ADCs and DACs provided on the SR 830 phase sensitive detector (PSD) which operates off signals from the computer and exchanges data with it via a GPIB bus. This also controls the frequency through a connection to the RF synthesizer, whose output is fed to a mixer for modulation at an AF of 380 Hz. This is obtained as an output from the SR 830, and is also used internally as the reference for the PSD. A DAC allows the RF power level (PL) to be set via a voltage applied to a VCA in the mixer. The level of feedback (FB) is similarly controlled by use of a second VCA (see figure 5). The modulated RF signal is applied to a power amplifier and thence to the coil and a 15 dB 150 W attenuator, whence it flows to earth through an approximately 50 Ω resistance (not shown). A RF detector connected to the top end constitutes the front end of the feedback loop, through an ADC on the SR 830 and on to the computer via the bus. The signal is compared with a calibration curve and an error signal is developed which is fed back via the bus to the mixer through a second DAC and onto the power amplifier to complete the loop. In the diagram the circles containing crosses represent points at which resistors have been added in earth return lines to suppress earth loops. An oscilloscope monitors the level of the modulated RF signal from the mixer, and the output from the PSD. The pump which circulates the sample is not shown as are not the mains and earth connections. But this pump, the light intensity monitor, the lamp and its power supply are all fed from a single connection to mains. A second mains connection goes to the computer and its monitor whilst a third connects to all other units. Not all power supplies are shown. Great care was taken to separate the earth connections to 'clean' and 'dirty' units (see text).

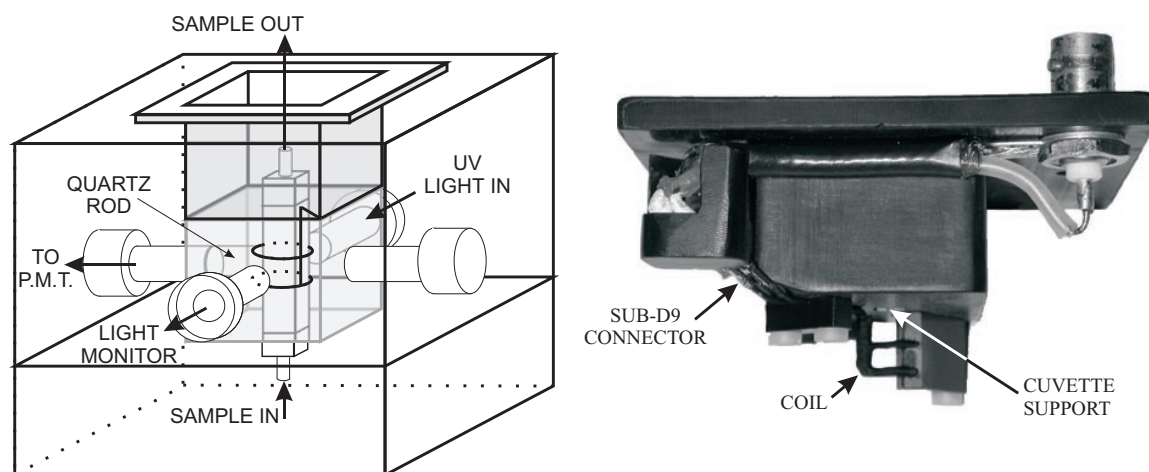


Figure 3. An exploded view of the delrin spectrometer block. This diagram is semi-schematic. It shows where the lower block is divided into two parts to aid assembly but not the details of how this is done. Similarly, the lid is shown in this diagram in simplified form but a photograph of the real one is also provided. In this the rigid support of the RF coil can be seen, as can the square hole into which the upper part of the cuvette plugs. The size can be judged by reference to the standard BNC connector via which the RF is applied. The diagram shows that a similar hole locates the base of the cuvette.

generator, which is the source of the AF used both to provide its reference signal and to modulate the RF, and analogue-to-digital (ADC) and digital-to-analogue (DAC) converters. The experiment is controlled by a central computer through a GPIB bus, using these converters.

As will be seen below, up to 200 W of RF power is applied to a coil, which surrounds the sample, and a series load. This, together with the continuous sweep of frequency required, places stringent demands on apparatus design and on the suppression of artifacts due to electrical pick-up.

The whole spectrometer is under computer control using software written in house, implemented in *Visual Basic*. This also allows all aspects of the experiment to be monitored.

2.2. The spectrometer block (figure 3)

At the heart of the experiment lies a narrow sample tube held within the coils of a two-turn Helmholtz pair, via which the radiofrequency radiation is applied. Both are held rigidly within a block drilled to allow flow of the sample, to minimize depletion of the photo-active material, and to allow ingress and egress of light. The excitation light passes through the sample and out, whilst the fluorescence light is detected in an orthogonal direction. The former is conducted to the block via a liquid-filled UV transmitting light guide (Oriel) which plugs rigidly into it. The fluorescent light is conducted by a similar second light guide to a photomultiplier tube (PMT, Hammamatsu R928) for detection; a short length of silica with optically polished ends abuts the sample tube and conducts the fluorescence efficiently into the light guide. Use of the milled block and light guides establishes a rigid and appropriate geometry for the experiment that could be accomplished otherwise only by use of an optical table. It makes the experiment compact, an important feature in minimizing electrical pick-up, and comparatively unaffected by vibration. It further allows us to place the whole of the block within an annealed mu-metal box to minimize stray magnetic fields, due to the geomagnetic field or laboratory sources, at the sample. This is essential for straightforward analysis of the experimental results. Since electrical pick-up is a source of possible systematic error, the whole of the block and the mu-metal box are further contained in an earthed copper shield.

The block is milled from black delrin and consists of a base into which a recess in its lid projects so as to locate the coil that is mounted onto it accurately. The base is in two parts, which fit snugly together, to allow assembly of the inner parts. The sample tube is a custom-made suprasil cuvette of $3 \times 3\text{mm}^2$ inner dimensions, and $5 \times 5\text{mm}^2$ outer dimensions, with tubular ends to which plastic tubes are attached to allow sample flow. These are fastened to the block to prevent movement that might break the delicate cell. The bottom end of the cuvette rests in a milled tight-fitting square recess through which a hole is bored to pass the tubular end; an elastic ring placed around it on the outside of the block maintains its position. The top end is held within a similar tight-fitting square hole in the lid so that the geometry of the tube within the experimental area is rigidly defined. The cuvette sits within the Helmholtz pair and its small cross-section ensures that the field due to the coil is reasonably uniform over the sample. Calculations based on the dimensions of the coil and the sample tube suggest that any variation is 5–7%.

The coil is a low-inductance, low-capacitance, device made so that the strength of the field it produces varies little as the RF frequency is changed. It consists of two single turns of 0.8 mm diameter copper wire, 8 mm in diameter and 4 mm apart. Thin plastic spacers were introduced in the regions where the forward and return wires were close to reduce any parasitic capacitance, and the coil has uncompensated current only in the region of the turns, causing it to approximate Helmholtz behaviour. In the regions of these spacers the coil

was wrapped in cotton string and glued to provide mechanical rigidity once attached to its two fixing points in the block (see figure 3), and it was painted matt black to reduce light scattering and to aid heat dissipation. It was made demountable by attaching two gold-plated male pins from a Sub-D9 connector to the leads that mated with similar female sockets. These were placed in a break in the central lead of a short co-axial cable which was terminated at each end by a BNC connector fastened to the block to connect on the one hand to the RF source and on the other to the dummy load (see below).

The block was mounted inside an annealed mu-metal box with four 5 mm diameter openings, one of which was not used. Two allowed the aforementioned light guides to be introduced whilst a third, opposite the entry of the excitation beam, conducted light to a UV-enhanced photodiode. The signal from this was fed to a home-built comparator and thence to the power supply of the xenon lamp so as to stabilize the intensity of the light. The actual intensity of light falling on the sample was monitored continuously and the long term variation of the light flux was found to be less than 1%, allowing extensive signal averaging over many hours when needed with weakly fluorescing samples. One corner of the detachable cover was cut to allow all other connections to be made. Tests showed the residual field inside the box to be $<10 \mu\text{T}$, the lower limit of detection with the Hall effect device available.

2.3. Excitation and detection

Solution concentrations were adjusted to have low optical density to ensure an essentially uniform concentration of radicals throughout the sample. The solutions were pumped through the cuvette using a peristaltic pump with associated buffer volume to eliminate pulsing. Light from an Oriel 300 W lamp and power supply passed through a condenser and then through a water infra-red filter and a water-cooled band-pass glass filter chosen to select UV radiation whilst rejecting other wavelengths. It was then focused onto the 5 mm diameter light guide and conducted to the sample. The fluorescence from the sample was similarly taken to the photomultiplier tube via a narrow-band interference filter chosen to discriminate against scattered incident radiation, and between fluorescence arising from the exciplex and pyrene itself. The PMT is housed within a cylindrical mu-metal shield inside a light-tight anodized aluminium box, together with the filter holder; details of its base and its electrical screening appear later. It works in photocurrent mode and its bandwidth (10 kHz) imposes no significant limitation on the AF modulation frequency that can be used. Its voltage output is taken to the phase-sensitive detector (PSD), which has a $1\text{ M}\Omega$ input impedance, implying that this connection is a potential source of electrical pick-up. To reduce the antenna properties of the inter-connecting cable a $10\text{ k}\Omega$ terminator was introduced at the PMT end. Use of a single 50 cm double-shielded cable with a BNC connector proved to be less susceptible to pick-up than when an attempt was made to use the differential input of the PSD with a twisted pair of coaxial cables.

The phase of a lock-in detector is ideally set to optimize the signal in phase with the reference sine wave, but this is difficult to do if the signal is weak. In consequence both channels of the dual-channel PSD were used to provide simultaneous detection

and recording of the in-phase and out-of-phase signals from the PMT, which may not have been perfectly phased. The optimum signal could then be computed from this complete set of data.

The signal magnitude is critically dependent on the intensity of the fluorescent light reaching the PMT. As described above, a silica rod conducts the light from the cuvette to the light guide, and the other end of this guide is placed up against the optical filter, itself as close to the PMT as possible. Careful optimization produced a signal many times stronger than any due to pick-up, and greatly facilitated reducing this pick-up to a negligible magnitude.

2.4. The radiofrequency system

The design requirement is that the strength of the oscillating magnetic field generated by applying RF radiation to the coil should not vary as the frequency is swept through the range 1–80 MHz. This is accomplished using a non-resonant system but non-flatness in the coil circuit's response occurs due to the active nature of the electronics and the impossibility of attaining perfect matching. This is overcome by use of a feedback system, which involves careful calibration of its actuator (a voltage-controlled attenuator) on the input to the coil and a probe (a RF detector) on its output. A further requirement is that the AF modulation amplitude is independent of RF frequency. This has largely been accomplished, although some variation occurs that is compensated for by calibration.

2.4.1. The source and the coil. The RF is generated using a Programmable Test Sources PTS 500 frequency synthesizer, controlled from the computer via a GPIB board; it allows the frequency to be swept from 1 to 500 MHz in 0.1 Hz steps, and is stable to ± 0.1 Hz. The output is applied to the matched 50 Ω input of a Wessex Power amplifier (RC114-100) with a nominal power rating of 100 W_{RMS} in the frequency range 1–80 MHz. That this amplifier is restricted to frequencies below 80 MHz presently limits the frequency range that can be investigated, although it extends to 100 MHz at power levels below the maximum. The amplifier drives the coil in series with a Bird Electronics 150 W 20 dB 50 Ω attenuator, which provides a reasonably well matched termination to earth. The entire RF circuit is matched to 50 Ω without use of current transformers.

Since the circumference of the coil is much smaller than the wavelength of any RF frequency used, its response is similar to that with dc excitation. From its geometry, a field of about 0.225 mT is calculated at the centre for every 1.0 amp flowing through it, with a power consumption of 50 W. This field strength is of the order of that predicted to influence the chemical reaction. The 100% sine amplitude modulation halves the overall power dissipated in the load and 100 W_{RMS} was found to be the maximum usable under stable operation, but it corresponds to 200 W_{RMS} for the RF in the maximum of the AF modulation envelope.

The performance of the coil was calculated using the simplified equivalent circuit shown in figure 4. The coil itself had an inductance estimated at 50 nH, and a capacitance of less than a few pF, and was connected to the output of the amplifier and to the dummy load with 30 cm of 50 Ω coaxial cable, with

N-type connectors at these units and BNC ones at the coil. Since the length of the cables is substantially shorter than a quarter wavelength even at the highest frequencies used, the cables can be considered as elements with lumped parameters. With a capacitance of about 30 pF per metre, the capacitance and inductance of the cables is approximately 10 pF and 20 nH respectively. Application of a network analyser to the dummy load showed it to approximate a purely active impedance of 50 Ω over the frequency range 1–500 MHz. It was assumed that the output impedance of the amplifier was similar. These figures imply that the circuit has a resonant frequency of about 300 MHz, a wave impedance of 100 Ω and $Q \approx 1$. It is therefore a very broad band device. In agreement with this, direct measurement showed the frequency response of the coil within the block, together with its connecting cables, to be practically linear between 1 and 100 MHz, with no resonances and with a fall-off of only 1.4 dB across the range.

Essential to the analysis of our experiments is knowledge of the radiofrequency field strength at the sample. Over the frequency range employed, analysis of the equivalent circuit suggests that any current flow through the capacitance of the cables can largely be neglected so that the current flowing through the coil can be assessed directly by measuring the voltage drop across the load; in practice it is more convenient to measure this at the output of the 20 dB attenuator. The field is then calculated from this current and the known dimensions of the coil. At the maximum power of 200 W (see above) the current ~ 2.8 A and corresponds to a RF field of 0.63 mT. The power dissipation in the coil itself is about 0.25 W at maximum, implying ohmic heating of the sample is negligible, as is heating due to dielectric loss and light absorption.

The mechanical rigidity of the coil is itself important since its turns experience a non-zero average torque at the AF modulation frequency, and minute perturbations could lead to spurious modulation of the fluorescent light output through its effect on the RF field strength. Possibly more importantly, the firm suspension of the coil eliminates any modulation introduced by periodic mechanical interruption of a small portion of the exciting light beam.

2.4.2. Feedback and amplitude modulation. Measurement of the frequency response of the entire RF circuit, including mixing unit (see below), power amplifier, coil, load and cables, showed the power to vary nonlinearly over the range 1–80 MHz, by approximately 250% depending on the actual coil used. This variation was compensated for by use of negative feedback, using the circuit shown in figure 4. The feedback loop consists of a RF detector at the 20 dB output of the dummy load, the computer and two voltage-controlled attenuators (VCA), placed between the mixer chip where the modulated signal is created and the input of the power amplifier. They are controlled by the computer. The detector produces a dc output proportional to the RF power input and this is processed by the computer according to a careful pre-calibration before being fed back. The computer is connected to the analogue devices via DACs and ADCs available in the SR 830 lock-in amplifier. These have a voltage range of -10 to $+10$ V with a resolution of 10 mV; only positive dc voltage was used.

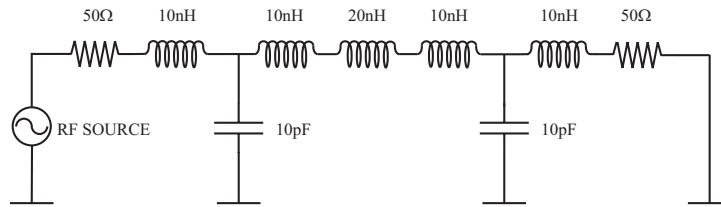


Figure 4. The equivalent circuit used to calculate the characteristics of the coil assembly. The RF coil is in the centre.

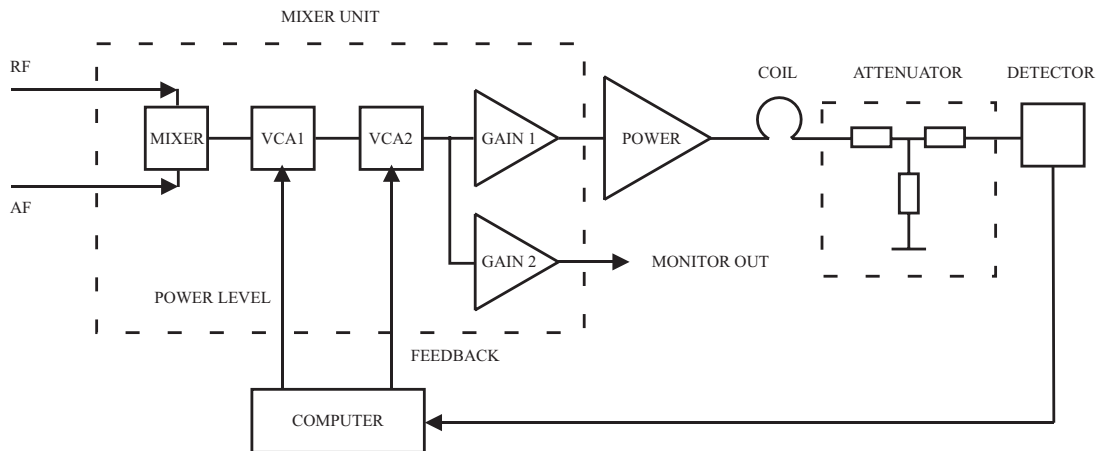


Figure 5. The feedback and modulation circuit described in the text. The signals shown as coming from the computer do so indirectly through the DACs on the phase sensitive detector. The mixer unit and the attenuator are contained in separate screened metal boxes.

Fixed amplitude RF and AF signals from their respective sources are first mixed in a single ‘mixer’ chip (AD 835 AN) to yield a low-level RF signal modulated at the reference frequency (380 Hz). This is conducted to the first of two identical voltage controlled attenuators (‘VCA 1,2’, TL 072 CN) which determines the output power via a signal from the computer. Its output is applied to the second VCA, which is used to compensate for the non-flatness of the frequency response. It constitutes the actuator of the negative feedback loop. A fixed gain pre-amplifier (‘GAIN1’, OPA 658P) set at 16 dB boosts the signal to the input level required by the power amplifier (‘POWER’ in figure 5). An identical pre-amplifier (‘GAIN2’) provides a signal to monitor the waveform and amplitude of this output by means of an oscilloscope. The amplified RF is applied to the coil (‘COIL’) and the dummy load that terminates the matched 50 Ω line (‘ATTENUATOR’). After tenfold attenuation the signal, now essentially decoupled from the high power circuit, undergoes detection to yield the dc output that is fed back, via the computer, to the second VCA.

All low-level active RF electronics are contained in a die-cast aluminium box with a separate power supply, and all inter-connecting coaxial cables are point-to-point matched 50 Ω ones. T-junctions are avoided to prevent cable interference effects and possible standing waves due to reflections.

RF detection is by a fast passive Schottky barrier rectifier (BAT 85) followed by a two-stage passive low-pass filter, which reduces ripple levels at the modulation frequency to below 1%. It is contained within a grounded aluminium box with isolated BNC connectors on the input and output. The parts of the circuit in which there exist high RF signal levels are carefully separated from those with none, with their common

leads connected to a single point. The dc signal return terminal is connected with the common point of the detector via a 10 k Ω resistor to suppress a possible ground loop.

2.4.3. Calibration of the feedback loop and of the modulation characteristics. The feedback loop was thoroughly calibrated, with a 50 Ω 100 MHz digital oscilloscope (Tektronix 2485B) connected via a 10 cm long co-axial cable used as a reference measuring device. Point-to-point connections without T-pieces were used throughout. The ac amplitude measured by the oscilloscope connected to the output of the power attenuator, with the detector disconnected, was compared with the dc voltage measured by the auxiliary ADC of the SR 830 connected to the output of the RF detector, with the oscilloscope disconnected. Calibration involved both the VCAs and the detector and was performed as follows.

- (i) With no AF modulation applied, attenuation versus control voltage characteristics were measured for both the feedback (FB) and the power level (PL) VCAs in the mixing unit, in the voltage range 1 to +10 V in steps of 0.1 V. These differed slightly between the two, but were typically sigmoidal with maximum slope around the centre of the voltage range and they had negligible frequency dependence. The VCAs were used in their region of maximum sensitivity ($\sim 3\text{--}7$ V). The characteristics were stored in the computer to allow fine control of the eventual RF power level, and the control voltage of the FB VCA was used to parametrize the RF signal level in a systematic fashion at further stages in the calibration process.

- (ii) Plots of the voltage amplitude registered by the oscilloscope (U_{scope}) and by the detector (U_{det}) were drawn as the FB VCA control voltage was varied between 0 and +10 V in 0.1 V steps at 11 frequencies in the range 1–101 MHz, with steps of 10 MHz. These two voltages were then plotted against each other to produce a good straight line graph which crossed the detector voltage axis at 215 mV. This represents the voltage drop across the detector diode.
- (iii) U_{scope} and U_{det} were then measured as a function of the RF frequency in 1 MHz increments across the range 1–100 MHz for 11 levels of RF power using VCA control voltages of 0–10 V in 1 V steps. The value of 215 mV was independent of frequency so that throughout the frequency range the actual detector voltage (U_{corr}) was obtained by adding this to the observed value. A universal calibration curve ($CAL(f)$) of the ratio (U_{corr}/U_{scope}) as a function of frequency was then obtained by averaging all the individual curves obtained at power levels in excess of 10 W, and stored in the computer. The difference between the average curve and each individual curve was less than 1% throughout the frequency range.
- (iv) Approximately 100% amplitude modulation was obtained by applying a 2.5 V amplitude AF signal to the mixer. The modulation depth (MD) was, however, observed to change with RF frequency, decreasing from 100% at 1 MHz to 90% at 80 MHz. This characteristic was again recorded. By empirical fitting to this curve a satisfactory correction for the fall-off in MD with frequency was found to be by multiplying the corrected detector signal by the factor $[2 - MD(f)]^{-1}$, where $MD(f) \leq 1$. Neither the maximum amplitude nor the MD of the modulated RF signal varied significantly with AF frequency.
- (v) The calibration curves obtained with AF modulation, taking U_{scope} as a measure of the maximum amplitude, were of the same shape as those measured without modulation, but the two differed by a factor of two (again empirical) in the magnitude of this voltage.

The calibrations allowed the RF power dissipated by the load to be calculated at all frequencies and hence the current flow through the coil and, from the known geometry, the magnetic field at the sample. The procedure was to measure the dc voltage at the output of the detector and to correct it for the voltage drop across the diode, to give U_{corr} , as above. This was in turn corrected for changes in the modulation depth, as described, and multiplied by two to allow use of the detailed calibration of the un-modulated system. The result was divided by the relevant figure from the calibration curve $CAL(f)$ to yield the amplitude of the RF at the output of the power attenuator:

$$U_0 = \frac{2U_{corr}}{(2 - MD(f))CAL(f)}.$$

The RMS power incident on the input of the 50 Ω 20 dB attenuator is then given by

$$P = \frac{\langle U^2 \rangle}{R} \times 100 = \frac{U_0^2}{2 \times 50} \times 100 = U_0^2$$

where the factor of 100 arises from the attenuation, P is in watts and U_0 is in volts.

The calibrations were monitored at maximum power over a period of weeks and remained unchanged.

The duty cycle of the feedback loop is synchronized with 55 ms pulses from the computer timer. An initial clock pulse advances the RF frequency and is followed by a second, 55 ms later to allow the system time to settle. The detector signal is then read, the incident power on the load is computed, and a new control voltage is applied to the second VCA, again allowing 55 ms for the system to settle before a third clock pulse initiates a final stage. This causes the detector signal to be read once more, the signal level to be re-checked, and a new correction cycle to commence if these measurements show it to be necessary. Since only small changes in frequency are normally used and the control curves of the VCAs and the calibration curve of the detector are known with sufficient precision, one cycle is usually sufficient to adjust the power level. One complete cycle occurs to set the power level at each value of the frequency, and once the power has been set the cycle does not recommence until the next frequency increment has been made. The minimum period between frequency steps is 300 ms. An apparently simpler way of building a feedback system, actuated from automatic measurement of RF amplitude with the digital oscilloscope, would be too slow.

The control and calibration curves were constructed on the basis of only 100 measurement points but they are smooth, and linear extrapolation between successive points is used to obtain intermediate values. The power level correction cycle is launched when the power differs by more than 2% from the level pre-set using the power level VCA. Overall the power level is maintained to 2–4% in the 1–80 MHz range and the overall accuracy of the power setting is about $\pm 5\%$. The feedback loop compensates very satisfactorily for the non-flatness of the frequency characteristics of the RF circuit and allows the coil to be replaced without the need for tedious re-calibration.

2.4.4. Suppression of electromagnetic interference. The experiment involves high levels of continuous wave RF, implying RF voltages up to 300 V_{pp} at maximum power and RF currents of several amperes in its various components. Furthermore, amplitude modulated RF is transmitted through space and is detected by any imperfect contacts, and spurious AF signals can arise in several parts of the apparatus. The PMT itself may act as an antenna, whilst the several nonlinear semiconductor devices are all potential detectors. Additional complications arise in the proximity of a high-power amplifier to a sensitive phase sensitive detector which has the envelope of the amplitude-modulated RF as its reference signal. The dimensions of the apparatus, which consists of more than ten stand-alone units and their associated mains leads and cables, are of the order of the wavelengths of the RF radiation used, which makes the interference problem particularly difficult through causing cables potentially to act as active circuit components and making the relative positions of the components critical. All mains connections are three-wire with a grounding pin, and all the commercial units used (except the PSD) have the signal return terminals of their input/output connectors connected to their chassis, creating multiple ground loops that act as antennae and introduce apparent signal sources into the system.

Suppression of interference consequently demanded a systematic approach throughout the apparatus. The copper box containing the spectrometer and its mu-metal shield was grounded to a single point, as was its lid. All connections other than mains leads and the PMT signal cable were made using high-quality double-screened (mesh+foil) digital grade coaxial cable of the shortest possible length, with the most sensitive further fed through copper mesh sleeves grounded to a single point and without contact to the connectors. The PMT, besides being magnetically shielded, was put into an electrostatic screen consisting of a solid copper enclosure connected to the negative high voltage terminal of the PMT via a 10 M Ω resistor. Its glass envelope was wrapped with a copper mesh sleeve connected to this. The metal box housing the PMT was made electrically tight by removing the anodized layer from all connecting surfaces and inserting copper mesh between them before tightening the screws which held it together. The box has no electrical contact with the PMT, its base or its power supply, and is grounded to a single point. The PMT is connected to a floating input on the phase-sensitive detector via a coaxial cable with two separate insulated screens separating the shield from the signal return path. One shield acts as the signal return path whilst the other is grounded. In this way the most critical parts of the apparatus where pick-up is concerned effectively float inside a grounded metal enclosure.

All cables and devices were positioned empirically and secured in place to minimize pick-up. Wherever possible all ground-signal return connections were single point connections in a tree configuration. 10 Ω or 10 k Ω resistors were placed in three points in the signal return lines from the RF detector, from the light intensity-monitoring and controlling amplifier and on the input to the PMT (this is a provision provided in the SR 830 model), to break possible earth loops. All metal surfaces and copper screens which might fortuitously make contact were enclosed in plastic to prevent possible ground loop formation. The ground connections from possibly 'dirty' units (the screen of the sample compartment, the case of the power amplifier, and the screening sleeves of the cables to the coil) were carefully separated from those to the 'clean' units (the PMT box, the shield of the PMT signal cable, the case of the SR830 and the screening sleeves of cables carrying low-level signals) and collected at different points before earthing through the mains supply (this is not shown in figure 2). High-power and noisy components and low-power high-sensitivity components were connected to the mains supply separately whilst a third independent mains source supplied the computer itself. Wurtz Electronics clamp-on cable ferrite chokes (7427111) were put on cables and mains leads which carried no RF. Through-space pick-up of the amplitude modulated RF signal by the lamp power supply leading to modulation of the light flux proved particularly irksome, but was overcome by removing it as far as possible from the rest of the apparatus and shielding it with aluminium foil.

The pick-up was reduced until its level fell below that of the dark noise of the PMT at full RF operating power, being monitored over 1 hour periods of signal averaging whilst the frequency was swept across its full range. A convenient check was provided by use of a fluorescing sample from which no RF spectrum was expected. Finally, no detectable interference

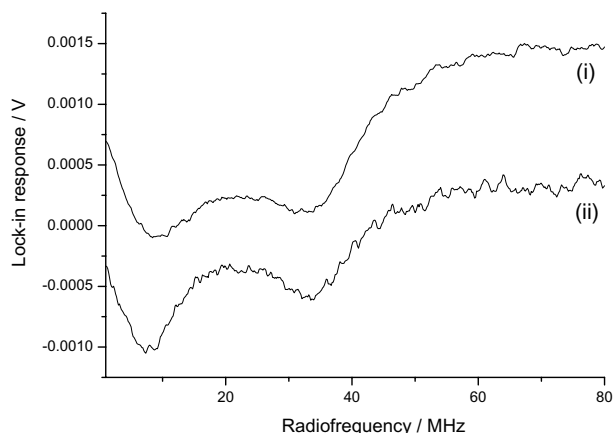


Figure 6. Specimen spectra of the radical pair produced on irradiating fully deuterated pyrene (10^{-4} M) in the presence of 1,3-dicyanobenzene (10^{-2} M) in a 1:9 mixture of cyanomethane and cyclohexanol (i) at high power (200 W into the load) and (ii) at double the gain at low power (50 W). The high-power signals have been displaced by 0.001 V for clarity, but the lower power ones are shown with respect to the true zero. As the power is decreased the lines sharpen but the signal-to-noise ratio deteriorates. The solvent mixture was chosen to stabilize the radical ion system whilst having a near-optimum viscosity for observing field effects.

caused by the equipment was experienced when running at full power by other very sensitive apparatus in the laboratory.

3. Sample results

A zero-field spectrum of the exciplex system obtained at full RF power across the frequency range 1–80 MHz is shown in figure 6(i); it has been averaged using 30 repeated scans, each scan taking 256 s. The conditions appear in the figure caption. Use of such a high power causes line-broadening but is often necessary in practice and it is used here to demonstrate the operation of the spectrometer under the most extreme conditions. The resonances observed in the spectrum are entirely as predicted theoretically, and occur at simple multiples or sub-multiples of the hyperfine frequencies [6, 7]. At lower RF levels the peaks sharpen, as shown in figure 6(ii), obtained with averaging, as above. The signal is, however, about half as strong at this power level. The absolute magnitude of the effect is small, and this limits the signal-to-noise ratio, which, however, remains adequate to detect the main features even when the RF power is reduced. The results from experiments conducted on isotopically substituted exciplex systems have been submitted for publication elsewhere [15].

4. Summary

A novel spectrometer has been described to observe the ESR spectrum of transient spin-correlated radical pairs in zero field and to study the effects of RF radiation on free radical combination reactions. It required careful design and assembly due to the necessity to sweep high power RF across a wide frequency range. This goal has, however, been attained. The experiment promises to give new insight into the nature and dynamics of radical reactions that occur widely in chemistry and biology, and it shows that such processes can indeed

be affected by RF fields. This may have physiological implications especially where environmental fields from a variety of sources are concerned and it may allow the control of chemical reactions by novel means.

Acknowledgments

We are grateful to Professor P Styles for advice, to the EPSRC for financial support (grant No GR/M 11332), and to the Royal Society for the award of a Dorothy Hodgkin Fellowship to CRT. The work forms part of the INTAS project 99-01766. It could not have been completed without the skill and craftsmanship of the members of the electronic and mechanical workshops in the Physical and Theoretical Chemistry Laboratory or advice from equally skilled technicians in Novosibirsk.

References

[1] Steiner U and Ulrich T 1989 *Chem. Rev.* **89** 51–147

- [2] Timmel C R, Till U, Brocklehurst B, McLauchlan K A and Hore P J 1998 *Mol. Phys.* **95** 71–89
- [3] Eveson R W, Timmel C R, Brocklehurst B, Hore P J and McLauchlan K A 2000 *Int. J. Radiat. Biol.* **76** 1509–22
- [4] Stass D V, Tadjikov B M and Molin Yu N 1995 *Chem. Phys. Lett.* **235** 511–16
- [5] Woodward J R, Jackson R J, Timmel C R, Hore P J and McLauchlan K A 1997 *Chem. Phys. Lett.* **272** 376–82
- [6] Stass D V, Woodward J R, Timmel C R, Hore P J and McLauchlan K A 2000 *Chem. Phys. Lett.* **329** 15–22
- [7] Timmel C R and Hore P J 1996 *Chem. Phys. Lett.* **257** 401–8
- [8] Canfield J M, Belford R L, Debrunner P G and Schulten K 1996 *Mol. Phys.* **89** 889–930
- [9] Weller A, Staerk H and Treichel R, 1984 *Faraday Discuss. Chem. Soc.* **78** 271–8
- [10] Strach S J and Bramley R 1983 *Chem. Rev.* **83** 49–82
- [11] Strach S J and Bramley R 1984 *J. Magn. Reson.* **56** 10–32
- [12] Strach S J and Bramley R 1984 *Chem. Phys. Lett.* **109** 363–7
- [13] Jeschke G and Schweiger A 1996 *Chem. Phys. Lett.* **259** 531–7
- [14] Thayer A M and Pines A 1987 *Accounts Chem. Res.* **20** 47–53
- [15] Timmel C R, Woodward J R, Hore P J and McLauchlan K A *Phys. Rev. Lett.* submitted